1973

An optimum low frequency digital communications receiver

Doherty, James Thomas

: Massachusetts Institute of Technology

AN OPTIMUM LOW FREQUENCY DIGITAL COMMUNICATIONS RECEIVER.

James Thomas Doherty

AN OPTIMUM LOW FREQUENCY DIGITAL COMMUNICATIONS RECEIVER

by

James Thomas Doherty Jr.

B.S., U.S. Coast Guard Academy

(1969)

SUBMITTED IN PARTIAL FULFILLMENT OF THE

REQUIREMENTS FOR THE DEGREES OF

ELECTRICAL ENGINEER

AND

MASTER OF SCIENCE

at the

MASSACHUSETTS INSTITUTE OF TECHNOLOGY

June 1973

AN OPTIMUM LOW FREQUENCY DIGITAL COMMUNICATIONS RECEIVER

by

James Thomas Doherty Jr.

Submitted to the Department of Electrical Engineering on 11 May 1973 in partial fulfillment of the requirements for the Degrees of Electrical Engineer and Master of Science.

ABSTRACT

In the Low Frequency (LF, 30-300 kHz) band of the electromagnetic spectrum, one finds many digital communication systems. At these frequencies, atmospheric noise, predominantly caused by radiation from lightning discharges, is the dominant noise which corrupts the signal. When viewed at the output of the receiver's bandlimiting filter, the noise waveform is very definitely non-gaussian. Since the noise is non-gaussian, it would be difficult to design an optimum communication receiver without knowledge of specific properties of the noise.

A model for bandlimited low frequency atmospheric noise, which accurately fits both the first order probability density and the time structure of observed noise waveforms, and which is well suited for digital computer simulations, has been developed by Feldman.[1] In the development of this model, a statistical dependence between the noise waveform on one bandlimited frequency channel and the envelope of the noise on a disjoint, but nearby, frequency channel was identified and incorporated into the model. On the basis of this property, a design for a two channel low frequency communication receiver, which makes nearly optimum use of the joint channel information, was proposed.

THESIS SUPERVISOR: Amar G. Bose

TITLE: Professor of Electrical Engineering

This work has addressed itself to the task of simulating the joint channel receiver and testing its performance relative to a single channel linear correlation receiver. Both receivers operate in the presence of low frequency atmospheric noise, as simulated by the above mentioned noise model.

The modem was assumed to be coherent phase shift keying, with the signal set consisting of $\pm$ A cos $2\pi f_c t$. The criterion for performance comparison was an estimate of probability of error per binary bit of information received. Our results show that, with the dual channel receiver, performance improvements of more than an order of magnitude can be expected during periods of severe non-gaussian noise activity. Suggestions for further research with this receiver design are presented in the last chapter of this work.

ACKNOWLEDGMENT

To acknowledge all those who helped in the successful completion of this research would be an almost impossible task. However, the following is a partial listing of those who most strongly influenced the outcome of this work:

Patti, Michael and David, who gave all the love and understanding necessary to help her husband, and their father, through two years of graduate school;

LCDR Donald A. Feldman, USCG, who developed the noise model and receiver design used in this research;

all the officers and men of the U.S. Coast Guard, with whom I have had the pleasure of serving these past eight years, providing all my formal education beyond the high school level;

the staff and "hackers" of the PDP-1X computer, who provided computer time, programming and system help;

and, most important, Professor Amar Bose, who gave unstintingly of his time in patiently guiding me through to the successful completion of this thesis.

TABLE OF CONTENTS

LIST OF FIGURES

LIST OF TABLES

Chapter 1

INTRODUCTION

In the Low Frequency (LF, 30-300 kHz) band of the electromagnetic spectrum, one finds many digital communication systems. At these frequencies, the dominant noise encountered is atmospheric noise, which is predominantly caused by radiation from lightning discharges. Since individual discharges tend to dominate the noise waveform observed at the output of a bandlimiting filter, we must assume that the noise cannot be statistically described as a gaussian noise process. Clearly then, one cannot hope to build an optimum communication receiver without some knowledge of the specific non-gaussian characteristics of the low frequency atmospheric noise.

The research reported in this work will demonstrate one particular realization of a near optimum binary digital communication receiver which is based upon the observed characteristics of bandlimited atmospheric noise. In this chapter, we will discuss the actual atmospheric noise and a model for that noise which can be used in digital computer simulations.

In Chapter 2, we present a receiver design which uses a second disjoint frequency channel to provide more information about the noise which corrupts the signal.

We will show that this receiver makes nearly optimum use of the joint channel information. We will also compare this receiver to a single channel linear correlation receiver.

Chapter 3 is devoted to an explanation of the calculations necessary to relate the analog system to the digital simulations of the proposed receiver. Our criterion for evaluation of receiver performance will simply be an estimate of the probability of error per bit of binary information received.

In Chapter 4, we will present the results of our simulations of both the single channel and joint channel receiver models, in the presence of the simulated low frequency atmospheric noise. We will give bounds on the accuracy of our results and explain some of the problems encountered in carrying out the simulations.

Finally, Chapter 5 will give a summary of this research, the conclusions reached, and some suggestions for further research.

1.1 Low Frequency Atmospheric Noise

There have been many observations of bandlimited low frequency atmospheric noise, which have led to descriptions of the noise characteristics (for example, see 1,2), but all note that the noise waveform is an extremely non-gaussian process. At individual times,

the noise waveform is dominated by peaks of high instantaneous energy, with several peaks occasionally occurring rapidly enough to yield a seemingly continuous burst of high energy.

Each high energy peak can be related to the radiation released from a lightning discharge. There are two basic strokes in each discharge: the leader stroke with an average length of about 1 msec and centered in frequency about 30 kHz, and the return stroke with a length of about 100-200 usec and centered about 3-8 kHz. In many instances, there are complicated repititions of these two basic strokes which yield the continuous noise burst behavior noted above. Between high energy bursts, the noise waveform can be accurately characterized as a low level gaussian waveform.

Feldman[1] reported that the following observed properties of the bandlimited noise waveform were useful in developing a model for this noise: First, at low frequencies, the noise is highly dependent upon local weather conditions. Second, above a certain threshold, the first order joint statistics of the noise waveform in one frequency channel and the noise envelope in a second disjoint, but nearby, frequency channel are statistically dependent. Third, the bandlimited waveform has an average power spectral density which is proportional to the square of the narrow-band filter's frequency

response. And fourth, for bandwidths of 1 kHz or larger, the process can be considered uncorrelated beyond 1 msec. In the next section, we will present the noise model which Feldman subsequently developed.

In his analysis of atmospheric noise, Feldman[1] noted that one of four basic weather/noise conditions is sufficient to describe the noise at any particular time. These noise conditions are quiet, tropical, frontal, and quiet night. Quiet corresponds to a stable air mass, with little thunderstorm activity, in the vicinity of the receiver. Tropical conditions exist when warm, moist, unstable air, with much thunderstorm activity, is present near the receiver. Frontal corresponds to the passage of a front in the vicinity of the receiver. Quiet night represents a transitional period between quiet and tropical conditions. The order of severity varies from nearly gaussian to nearly continuous high energy burst behavior for quiet, quiet night, tropical, and frontal conditions, respectively.

1.2 Noise Model

The model for bandlimited low frequency atmospheric noise, $y(t)$, which we will consider in this work is the following:[1]

$$y(t) = n_1(t) + a(x(t))n_2(t), \qquad (1.1)$$

where $n_1(t)$ and $n_2(t)$ are statistically independent

gaussian processes and $n_1(t)$ represents the low level gaussian background process. The quantity $a(x(t))n_2(t)$ represents the high energy bursts of noise due to lightning discharges, and $x(t)$ is a two-state Markov process with a time-varying rate parameter. The two states of $x(t)$ turn on and off the high energy noise component. Whenever $x(t)$ is in the "off" state, $a(.)$ is zero, and whenever $x(t)$ is in the "on" state, $a(.)$ becomes a random number, which is constant over the time interval that $x(t)$ remains in the "on" state. Each time $x(t)$ changes from "off" to "on," a new random value for $a(.)$ is generated, and $a(.)$ remains constant until $x(t)$ turns it off.

This model incorporates the observed dependence between the noise waveform on one channel and the envelope of the noise on a second disjoint, but nearby, frequency channel by assuming that $a(x(t))$ remains independent of frequency. Thus, it follows that the model for the envelope of the bandlimited noise, $v(t)$, on a second frequency channel is

$$v(t) = v_1(t) + a(x(t))v_2(t), \qquad (1.2)$$

where $v_1(t)$ and $v_2(t)$ are statistically independent Rayleigh processes.

It must be noted that this noise model cannot exactly specify the short-time structure of the actual

atmospheric noise. However, since LF receivers use sharp bandlimiting filters, with long observation times, this noise model is sufficient because it accurately simulates the average behavior of the noise over these relatively long time intervals. The model is based on the first order probability density of the bandlimited noise. In addition, properties of a(x(t)) are such that the model accurately simulates the actual long-time time structure of the noise.

Each of the four noise conditions (quiet, quiet night, tropical, and frontal) can be simulated with the noise model simply by varying the parameters used in the generating mechanism. In this research, all four noise conditions were simulated extensively using a canonic noise generator and table of associated parameters given in Figure 3-11 and Table 3-1, respectively, of reference (1). Since these two items are of vital importance to this research, they have been included as Figure 1.1 and Table 1.1 of this report. The results of the simulations, conducted in this research project, are given in Chapter 4 of this work.

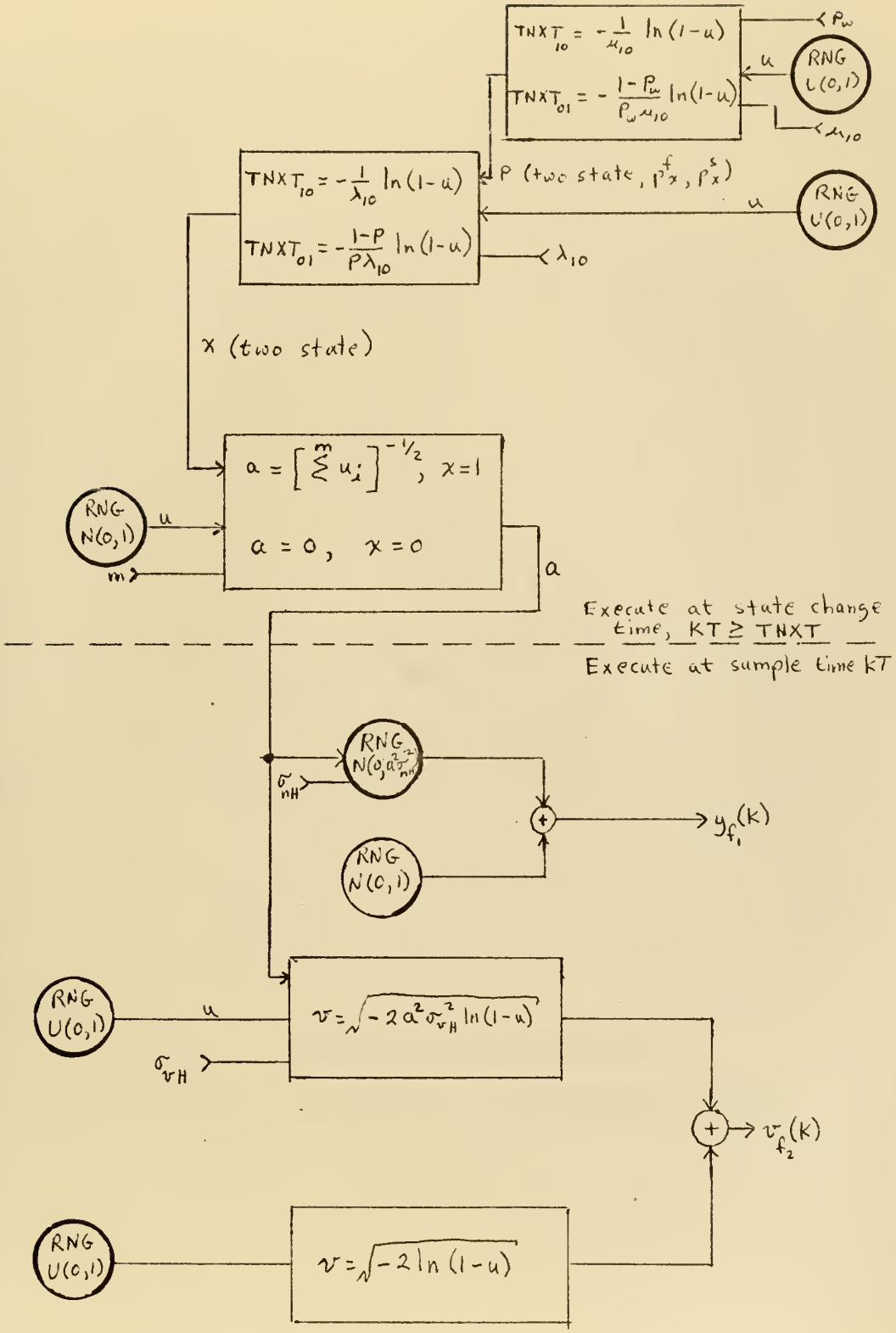

Figure 1.1 Canonic Noise Generator

Condition	f_c (kHz)	BW (kHz)	σ_{nH}	σ_{vH}	m	$\lvert\bar{g}\rvert$	$\lvert\bar{RF}\rvert$	$\bar{v}$	$\bar{E}$	$\bar{g}^2$	$\bar{RF}^2$	$\bar{v}^2$	$\bar{E}^2$	max	$\bar{P}_x$	P_x^f	P_x^s	I_w	μ_{10} (Hz)
Quiet	65	10	1.8		2	1.07	0.95			4.0	4.12			92	0.11	0.11	0.11		
Quiet	65	1	2.6		2	1.19	0.96			9.06	4.25			92	0.11	0.11	0.11		
Quiet	83	1		2.22	2			1.62	1.30			9.92	13.9	120	0.11	0.11	0.11		
Quiet night	65	1	1.23		2	1.66	1.30			10.9	12.6			100	0.5	0.75	0.25	0.5	1.0
Quiet night	85	1		1.34	2			2.71	3.09			18.5	25.6	134	0.5	0.75	0.25	0.5	1.0
Tropical	65	10	0.6		1	2.51	2.12			74.8	63.2			250	0.75	0.99	0.27	0.66	0.6
Tropical	65	1	0.54		1	2.23	1.91			57.0	47.8			250	0.75	0.99	0.27	0.66	0.6
Tropical	83	1		1.28	1			6.16	6.36			289.	275.8	285	0.75	0.99	0.27	0.66	0.6
Frontal	100	20	3.5		1	12.78	11.5			2300.	1936.			1000	0.9	0.99	0.15	0.89	0.2
Frontal	65	1	4.1		1	11.3	11.5			853.	918.			500	0.9	0.99	0.15	0.89	0.2
Frontal	83	1		4.6	1			22.2	27.0			2840.	5470.	700	0.9	0.99	0.15	0.89	0.2
Quiet night	14	1	0.3		1	1.21	1.13			4.84	6.0			40	0.45	0.66	0.24	0.5	1.0
Tropical	14	1	0.45		1	1.81	1.66			22.2	20.0			107	0.65	0.86	0.44	0.5	1.0
Tropical	14	1	1.05		1	3.52	3.33			102.	102.			200	0.8	0.99	0.15	0.84	0.3

NOTES: $\sigma_{nG} = \sigma_{vG} = 1$, $\lambda_{10} = 850$ Hz

Table 1.1 Noise Model Parameters

(braces and arrows indicate parameters we used)

Chapter 2

RECEIVER

In Chapter 1, we presented some properties of the bandlimited low frequency atmospheric noise, the noise which corrupts signals in low frequency radio communication systems. We also presented a model, suitable for simulation on a digital computer, which accurately represents that noise. The low frequency atmospheric noise, when viewed at the output of the receiver's bandlimiting filter, has been observed to be extremely non-gaussian. However, we presented several properties of the noise which can be exploited in the design of a nearly optimum receiver.

In this chapter, we will present a model for a phase coherent linear correlation receiver. We will show that this is the optimum receiver for signals corrupted by white gaussian noise, but it is not necessarily optimum when the noise is non-gaussian. We will also present a receiver design, based on the specific observed properties of bandlimited low frequency atmospheric noise, which should yield nearly optimum performance. However, implementation of the new design is approximately twice as complicated as implementation of the linear correlation receiver.

2.1 Modulation-Demodulation Scheme

Since the basic purpose of this research is to compare the performance of a new receiver design with that of a standard receiver design, we have chosen a computationally simple modulation-demodulation scheme. We postulate, since we are comparing both receivers under the same set of conditions, that our results in this somewhat idealistic case will still be representative of the results we would expect in a more realistic case.

In the simplest case, the receiver must decide whether or not a signal is present. In a slightly more complicated, and more realistic, case, the receiver must decide between two signals. We have thus chosen our signal set to contain two signals, each containing the same amount of energy. This signalling scheme, in which one signal is the negative of the other, is known as antipodal signalling.[3]

Since only a limited amount of data was analized in the development of the noise model, we have parameters available to model the bandlimited noise waveform only under certain frequency and bandwidth constraints. Keeping these constraints in mind, we must satisfy the not unrealistic condition that all radiated signal energy be confined to the frequency band centered at 65 kHz, with a bandwidth of 1 kHz.[1] (see Table 1.1)

This means that in the baseband, the lowpass region of the frequency spectrum, our signals must contain no energy in any frequency component greater than 1 kHz. In order to satisfy this constraint in a simple manner, we have chosen our baseband signal set to consist of

$$s_b(t) = \pm A, \tag{2.1}$$

and thus, since A is a constant, the frequency spectrum of each of our baseband signals consists only of an impulse at the frequency origin.

However, we are restricted to a frequency band centered not at the origin but at 65 kHz for transmission. Therefore, we must modulate our signals up to this passband. To do this, we simply allow our signals to ride on a cosine carrier of frequency 65 kHz; and thus our passband signal set becomes

$$s(t) = \pm A \cos 2\pi f_c t, \tag{2.2}$$

where $f_c = 65$ kHz.

At this point, we will separate the members of our transmitted signal set, thus:

$$s_0(t) = A \cos 2\pi f_c t, \tag{2.3a}$$

which represents a binary zero being sent, and

$$s_1(t) = -A \cos 2\pi f_c t, \tag{2.3b}$$

which represents a binary one being sent. From the above, it is clear that

$$s_1(t) = -s_0(t) = A \cos (2\pi f_c t + \emptyset), \tag{2.3c}$$

where $\phi = \pi$. Thus, we see that our signal set consists of two phase shift keyed (PSK) signals.

In general, this is not a practical way of signalling by radio communication systems due to the high voltage switching transients which occur when reversing phase. However, for signals corrupted by gaussian noise, the optimum PSK demodulator performs 3 db better than the optimum frequency shift keyed (FSK) demodulator, where binary FSK signal sets consist of

$$s_0(t) = A \cos 2\pi f_0 t \qquad (2.4a)$$

and

$$s_1(t) = A \cos 2\pi f_1 t, \; f_1 \neq f_0. \qquad (2.4b)$$

Furthermore, low frequency signalling schemes which approach PSK in performance have been developed, and it is felt that analysis of a PSK model will give an indication of performance to be expected in these new schemes.[2]

If there were no noise present, the optimum demodulator would filter out all signals but those in the passband, monitor the received signal, compare it with a reference signal (which is an exact replica of either $s_0(t)$ or $s_1(t)$), and decide which signal was sent. However, there invariably is noise present, which in the simplest form is additive white gaussian noise. Other forms of noise, such as a random attenuation of the signal or a random phase shift, may exist. We will,

however, restrict ourselves to the additive noise case. The reasons for this will be given in the next section, where we explain the linear correlation receiver.

2.2 Linear Correlation Receiver

In almost any text on communication theory, one can find a description of a linear correlation receiver (see, for example, 3,4,7). In Figure 2.1, we show a linear correlation receiver which decides which of two arbitrary signals has been received. In Figure 2.2, we show how that receiver can be simplified for the case of antipodal signals, the case we are considering.

Let us now assume that the received signal, r(t), consists of the following (see Figure 2.2):

$$\begin{aligned} r(t) &= s(t) + n(t) \\ &= \pm A \cos 2\pi f_c t + n(t), \end{aligned} \tag{2.5}$$

where n(t) is the additive white gaussian noise. We will assume that n(t) is a stationary, zero mean process, with autocorrelation function,

$$R_n(t_1-t_2) = \frac{N_0}{2} \delta(t_1-t_2), \tag{2.6}$$

where $\delta(.)$ is the Dirac delta function. From this, it is clear that

$$\begin{aligned} r_1(t) &= \pm A^2 \cos^2(2\pi f_c t) + A\, n(t) \cos 2\pi f_c t \\ &= \pm \frac{A^2}{2} (1 + \cos 4\pi f_c t) + A\, n(t) \cos 2\pi f_c t, \end{aligned} \tag{2.7}$$

and

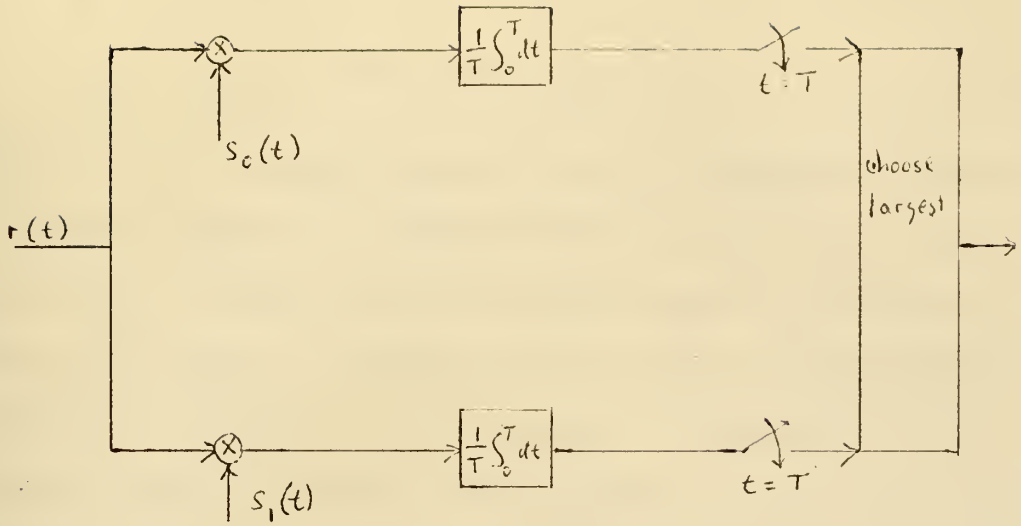

Figure 2.1 General Linear Correlation Receiver

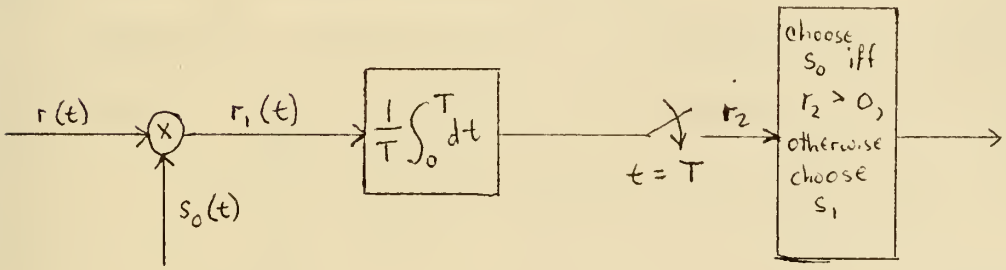

Figure 2.2 Linear Correlation Receiver-Antipodal Signals

$$r_2 = \frac{1}{T}\int_0^T \left[\pm \frac{A^2}{2} (1 + \cos 4\pi f_c t) + A\, n(t) \cos 2\pi f_c t \right] dt$$

$$= \pm \frac{A^2}{2} + \frac{1}{T}\int_0^T A\, n(t) \cos 2\pi f_c t \, dt, \qquad (2.8)$$

where we have assumed that T, the bit length or length of time in which the receiver must decide which signal was sent, is equal to an integral number of periods of the cosine wave. Actually, this is not a restrictive assumption because the bit length is typically much longer than the length of one period of the cosine wave.

It is clear, since n(t) has been defined to be a gaussian random process, and since r_2 is the result of a linear filtering operation on n(t), that r_2 is a gaussian random variable.[3] Thus, we can completely specify the probability density of r_2 if we can find the first and second moments of r_2.

Taking the expected value of equation 2.8, we get

$$E(r_2) = \pm \frac{A^2}{2} + \frac{1}{T} E\left(\int_0^T A\, n(t) \cos 2\pi f_c t \, dt\right)$$

$$= \pm \frac{A^2}{2} + \frac{1}{T}\int_0^T A\, E(n(t)) \cos 2\pi f_c t \, dt$$

$$= \pm \frac{A^2}{2} . \qquad (2.9)$$

Taking the second moment, we obtain

$$E(r_2^2) = \left(\pm \frac{A^2}{2}\right)^2 \pm \frac{A^2}{2T} E\left(\int_0^T 2\, A\, n(t) \cos 2\pi f_c t \, dt\right)$$

$$+ \frac{1}{T^2} E\left(\int_0^T \int_0^T A^2\, n(t_1)\, n(t_2) \cos 2\pi f_c t_1 \cos 2\pi f_c t_2 \, dt_1 \, dt_2\right)$$

$$= (\pm \frac{A^2}{2})^2 + \frac{1}{T^2} \int_0^T \int_0^T A^2 E(n(t_1)n(t_2)) \cos 2\pi f_c t_1 \cos 2\pi f_c t_2 \, dt_1 \, dt_2$$

$$= (\pm \frac{A^2}{2})^2 + \frac{1}{T^2} \int_0^T \int_0^T R_n(t_1-t_2) A^2 \cos 2\pi f_c t_1 \cos 2\pi f_c t_2 \, dt_1 \, dt_2. \quad (2.10)$$

Substituting equation 2.6 into equation 2.10, using the properties of the Dirac delta function and trignometric identities, we obtain

$$E(r_2^2) = (\pm \frac{A^2}{2})^2 + \frac{A^2 N_0}{4T} . \quad (2.11)$$

Therefore,

$$Var(r_2) = \frac{A^2 N_0}{4T}. \quad (2.12)$$

Let us now define the following hypotheses:

$$H_0: \quad r(t) = s_0(t) + n(t), \quad (2.13a)$$

$$H_1: \quad r(t) = s_1(t) + n(t), \quad (2.13b)$$

which can be reduced to

$$H_0: \quad r_2 \text{ is } N(\frac{A^2}{2}, \frac{A^2 N_0}{4T}), \quad (2.14a)$$

$$H_1: \quad r_2 \text{ is } N(-\frac{A^2}{2}, \frac{A^2 N_0}{4T}), \quad (2.14b)$$

where N(m,n) denotes a gaussian random variable with mean m and variance n. In the case where either hypothesis is equally likely, implying that either a binary one or

a binary zero has been sent with equal probability, and where the penalty for making an incorrect decision is independent of whichever hypothesis is true, the decision rule for minimum probability of error is always: (see for example 3,4)

$$\text{Choose } H_0 \text{ if } r_2 > 0, \qquad (2.15a)$$

$$\text{Choose } H_1 \text{ if } r_2 < 0. \qquad (2.15b)$$

Thus, we have shown that Figure 2.2 is a model of the optimum receiver for our signal set when the noise is gaussian. However, we have not yet explained why we considered only additive noise. The concept of modelling the noise as inflicting a random attenuation upon the information part of the received signal does not change the optimum receiver structure for the signal set we have chosen. All operations remain the same, and the decision threshold remains at the origin; however, the probability of making an error will increase. Since the receiver structure remains the same, we feel that there is no necessity for considering attenuation.

However, the random phase shift is not easy to disregard. The primary cause of random phase shift noise is the fact that there is no way for our receiver model to insure that its reference oscillator will remain phase locked with the transmitter's oscillator. When unknown phase errors exist, the receiver loses its

ability to distinguish between $s_0(t)$ and $s_1(t)$. The receivers we have shown in Figures 2.1 and 2.2 are known as coherent phase receivers since they assume that their oscillators are perfectly locked to the transmitter oscillator. In reality, receivers are phase incoherent, and they are considerably more complicated than the simple coherent receivers we have shown. (see for example 3,4,5,6) We feel, however, since the object of this research is to perform a first test upon the dual channel receiver design, which we present in the next section, that we should only test the simple coherent phase receivers. Moreover, we feel that, since both receivers we are comparing will be coherent phase types, the results should be somewhat typical of the results to be expected in the incoherent phase case. Finally, if our results indicate significantly improved performance, then the more difficult, and more realistic, incoherent phase test would be justified.

2.3 Joint Channel Receiver

In the last section, we presented an optimum receiver for use when the corrupting noise is gaussian. However, when the noise is non-gaussian, we have no guarantee that an optimum gaussian receiver will yield optimum performance. With knowledge of the specific

non-gaussian nature of the actual noise encountered in low frequency radio communication systems, it should be possible to design a receiver which performs better than one which was designed for gaussian noise.

Receiver designs which have been tried, or proposed, for dealing with the non-gaussian high energy noise bursts generally involve some type of nonlinear device.[1,2] These receivers use clippers, hole punchers, and other similar nonlinear devices to limit the dominating effect of the high energy noise bursts.

Feldman[1] proposed another approach to the receiver design problem. He noted that, above a certain threshold, the noise waveform on the signal channel exhibited a statistical dependence upon the value of the noise envelope on a nearby, disjoint bandlimited frequency channel. His design exploits this characteristic in a nearly optimum manner by applying a multiplicative weighting function, based upon the inverse of the envelope measurement, to the signal channel. As it applies to this work, this receiver design, Figure 5-1 in reference (1), is shown here as Figure 2.3. It should be noted that this receiver is basically a modified linear correlation receiver.

The parameter v_t is critical to this design, and it is given by equation 4.32 of reference (1), which is

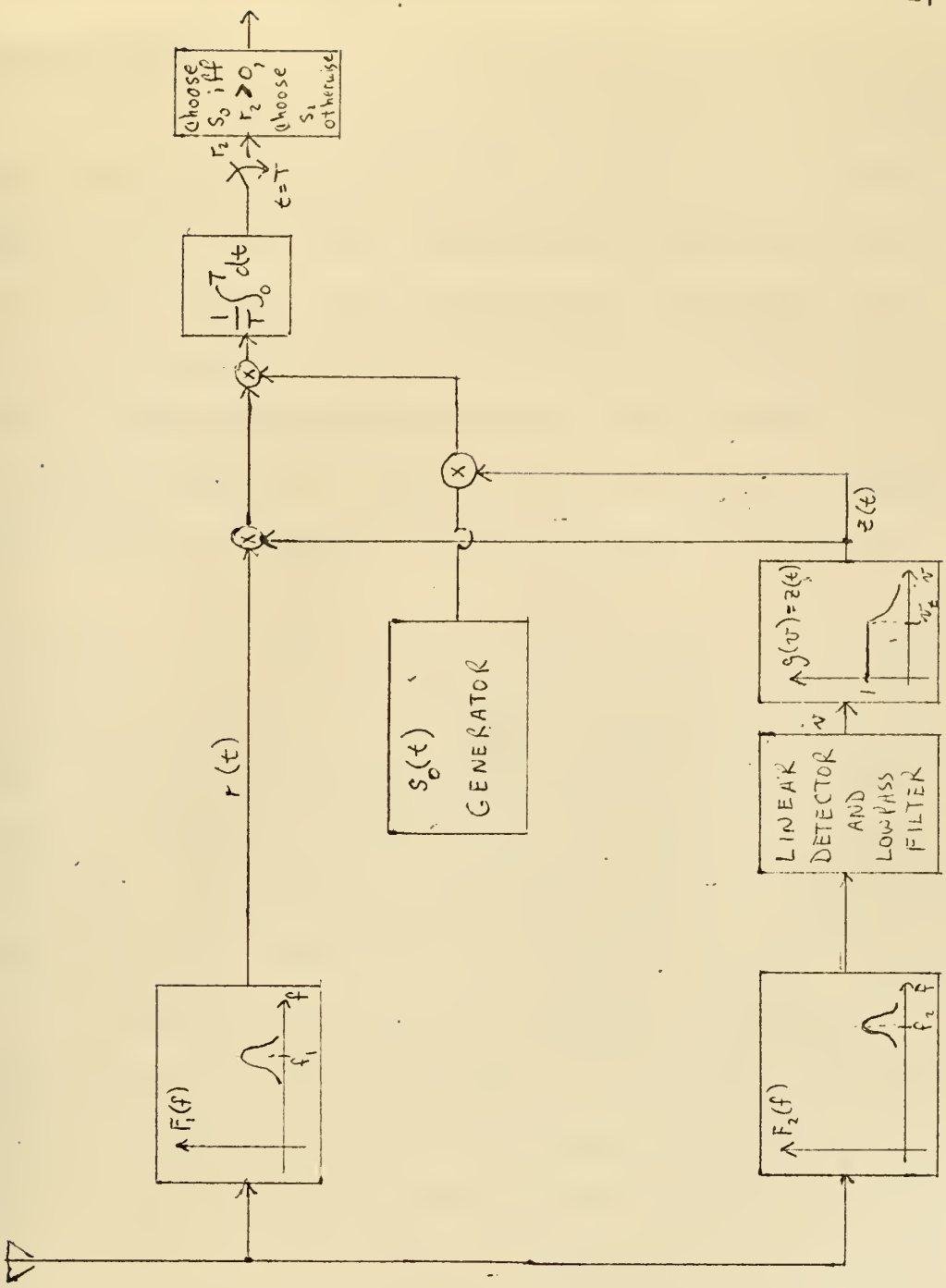

Figure 2.3 Dual Channel Receiver

repeated here:

$$v_t^2 = m \sigma_{nG}^2 \sigma_{vH}^2 / \sigma_{nH}^2, \qquad (2.16)$$

where the quantities on the right hand side are given in Table 1.1 of this work. Whenever the noise envelope on the second channel, v(t), exceeds the threshold value, v_t, there exists a statistical dependence between v(t) and the bandlimited noise waveform, y(t), on the information channel. Thus, a weighting function, z(t), given below, is applied to the information channel:

$$z(t) = \begin{cases} 1, & v(t) \leq v_t \\ v_t / v(t), & v(t) > v_t. \end{cases} \qquad (2.17)$$

We make no attempt to analytically verify that this inverse first order weighting function is indeed nearly optimum. Instead, we rely upon our results to verify this fact. The weighting function given in equation 2.17 above was first chosen as intuitively pleasing.

We verified our choice of weighting function experimentally. First, we point out that the object of the dual channel receiver is to reduce the problem from one in which we have a constant signal power level and a time varying, and unknown, (non-gaussian) noise power level to a problem in which the noise power level is kept constant and the signal power level is time varying in a known manner. Keeping this objective in mind, we conducted simulations for all four weather/noise

conditions, using various weighting functions. We simultaneously simulated an ad hoc receiver which was composed of a time varying signal, formed by applying the weighting function to only the information part of the received signal, and a gaussian noise process. We then chose the weighting function which yielded dual channel receiver performance closest to the performance of the ad hoc receiver. The final weighting function, z(t), thus determined is given by equation 2.17 above.

2.4 Chapter Summary

In this chapter we have presented the modem to be used in the receiver simulations of this work. In addition, we have presented an analysis of a linear correlation receiver which operates on binary antipodal signals that have been corrupted by additive white gaussian noise. We have also presented an improved design for a low frequency digital receiver, which utilizes information about the specific non-gaussian nature of the low frequency atmospheric noise to yield nearly optimum performance.

In the next chapter, we will explain some of the problems encountered in attempting a digital computer simulation of these receivers. We will also give examples of the calculations necessary to relate the digital simulation to the analog system being evaluated.

Chapter 3

SIMULATION CALCULATIONS

In this chapter, we will present the information necessary to relate our digital models of the noise and receivers to the actual analog systems we simulated. In the first section, we present the calculations necessary to convert the passband receiver model to baseband. In the second section, we calculate the probability of error for the simulated gaussian noise case. We also explain how we checked our receiver and noise model implementations on the computer. In Section 3.3, we give the calculations which relate the sampled data noise power spectrum to the analog noise power spectrum, in the white gaussian noise case.

3.1 Baseband Calculations

The received signals which we described in the last chapter were located, in frequency, in the receiver's passband. It is a well known fact that a signal must be sampled at least twice as fast as the most rapidly varying frequency component in the signal, in order to be able to recover the signal from the samples.

The highest frequency component of our received signal, r(t), given by equation 3.1, is the carrier frequency plus the bandwidth. The received signal, with

y(t) representing the bandlimited atmospheric noise, is

$$r(t) = \pm A \cos 2\pi f_c t + y(t). \qquad (3.1)$$

In our case, the carrier frequency is 65 kHz, and the bandwidth is 1 kHz; thus, the highest frequency component allowed in r(t) is 66 kHz. Therefore, to accurately recover r(t) from the samples, we must sample the signal at a sampling frequency of at least 132 kHz.

Bit lengths for low frequency digital communication receivers, the length of time in which the receiver must decide which of the two possible transmitted signals has been received, are usually about 20-50 msec.[1] For simulation purposes, we have chosen the lower end of this scale, in order to keep each simulation run as short as possible. Sampling at 132 kHz yields a time between samples of about 0.0076 msec, which we will round up to 0.01 msec for convenience. To simulate one bit of information, or 20 msec, at this sampling rate, we would require 2000 samples.

Our evaluation of receiver performance is based strictly upon an estimate of the probability of an error being made by the receiver in any particular bit of binary information received. In order to form this estimate, we have chosen the following approach: count the number of bits simulated, count the number of incorrect decisions made by the receiver, and divide the latter by the former. Olsen[5] recommends that if the maximum number

of bits we simulate is 1000, then the minimum probability of error we can estimate, with any accuracy, is 0.01. Further details about, and statistical bounds upon, our estimation procedure will be given in Chapter 4.

Based on the above, we feel that 1000 bits is the minimum number of bits we must simulate in order to derive meaningful results. In this case, to simulate the passband system, we will need 2,000,000 samples of the analog waveform, taken at a sampling interval of 0.01 msec. This is incredible, especially when it is realized that 1000 bits represent only 20 seconds of signalling. This is also impractical for various reasons: the first reason is the tremendous computation time needed, and the second is that our noise model is incapable of accurately simulating such fine time structure of the noise process as is required by this sampling rate.[1]

We have thus far ignored the one fact which allows us to solve this dilemma, the noise and transmitted signal are bandlimited. Therefore, we can accurately convert the passband system to a baseband system in which the maximum frequency component is 1 kHz. Clearly then, the maximum sampling rate necessary is 2 kHz, and the time between samples is 0.5 msec. Therefore, the number of samples per bit (20 msec bit length) is only 40, and the number of samples per 1000 bit simulation

run is only 40,000. Simulation of the baseband receiver is, of course, a much more tractable problem.

Any bandlimited process, random or deterministic, can be reduced to lowpass (baseband) processes. The procedure for doing this is rather simple, and it is presented in various references on communication theory (see, for example 3,4). We simply multiply the passband process by a cosine and/or sine of the carrier (bandcenter) frequency, and pass the resulting process through a low pass filter. A criterion for this procedure to work is that the bandwidth of the passband process must be much less than the carrier frequency.

Since the procedure which converts a passband process to a baseband process is actually a linear filtering operation, and since the received signal, r(t), is a linear combination of the transmitted signal, s(t), and the corruptive atmospheric noise, y(t), we can treat the conversion of each of these processes separately and linearly combine the results.

First we consider the transmitted signal (we consider only $s(t) = s_0(t)$, since $s_1(t)$ follows directly):

$$s(t) = A \cos 2\pi f_c t. \qquad (3.2)$$

Then the baseband process, by cosine conversion, $s_c(t)$, before low pass filtering, is

$$s_c(t) = A \cos^2(2\pi f_c t) = \frac{A}{2}(1 + \cos 4\pi f_c t), \qquad (3.3)$$

and, of course, after filtering,

$$s_c(t) = A/2. \tag{3.4}$$

Similarly, by sine conversion, we get $s_s(t)$:

$$s_s(t) = A\,(\cos 2\pi f_c t)(\sin 2\pi f_c t)$$

$$= \frac{A}{2} \sin 4\pi f_c t, \tag{3.5}$$

and after low pass filtering, this becomes

$$s_s(t) = 0. \tag{3.6}$$

Therefore, we see that in order to convert the transmitted signal portion of $r(t)$ to a baseband process, we simply must calculate $s_c(t)$.

We now consider the baseband conversion of $y(t)$, the bandlimited low frequency atmospheric noise process. By cosine conversion, before low pass filtering, we obtain $y_c(t)$:

$$y_c(t) = y(t) \cos 2\pi f_c t. \tag{3.7}$$

In a similar manner, before low pass filtering, $y_s(t)$ is

$$y_s(t) = y(t) \sin 2\pi f_c t. \tag{3.8}$$

After low pass filtering, $y_c(t)$ would be known as the in phase component of the baseband noise, and $y_s(t)$ would be known as the quadrature component.

At this point, we note that we have two baseband processes which have been generated from the bandpass received signal process, $r(t)$. These two processes are

$$r_c(t) = s_c(t) + y_c(t) = A/2 + y_c(t) \tag{3.9}$$

and

$$r_s(t) = s_s(t) + y_s(t) = y_s(t). \tag{3.10}$$

Since $r_s(t)$ contains no information about the transmitted signal, we would like to disregard it and perform a standard baseband correlation receiver operation upon $r_c(t)$ only. It can be shown[3] that if the spectrum of $y(t)$ is even over the bandwidth, then $y_c(t_1)$ and $y_s(t_2)$ are uncorrelated for all observation times t_1 and t_2. Further, if $y(t)$ were a gaussian process, then $y_c(t_1)$ and $y_s(t_2)$ would be independent. Then $r_s(t)$ would contain no additional information about either the signal or the noise, and it could be disregarded with no loss in optimality.

Bandlimited low frequency atmospheric noise is definitely non-gaussian, but Feldman[1] has noted that it has a spectrum which is determined solely by the band-limiting filter's frequency response squared, which we assume to be even over the bandwidth. Therefore, we can state that $y_c(t_1)$ and $y_s(t_2)$ are indeed uncorrelated for all time instants t_1 and t_2. Moreover, we assume that the statistical dependence between $y_c(t_1)$ and $y_s(t_2)$ is sufficiently small so that we can ignore $r_s(t)$. We feel that this is not a limiting assumption, especially when viewed in the light that it allows us to simulate a baseband receiver as opposed to the nearly impossible task of simulating the passband receiver. We also invoke the fact that we are comparing the results of two

receivers under the same set of conditions to justify our assumption that ignoring $r_s(t)$ is of little consequence.

Now that we have transformed our received signal into a baseband signal, we will proceed with the simulation of a baseband receiver. The received signal is now represented by equation 3.9. As a practical matter, we generated $y_c(t)$ on the computer by sampling $y(t)$ at twice its bandwidth and multiplying the samples by the value of $\cos 2\pi f_c t$ at the sample times. In the next section, we will state how we tested our receiver and noise model implementations on the computer by calculating the probability of error in the gaussian noise case.

3.2 Receiver Implementations

In the last section, we described the manner in which we converted an untractable passband receiver simulation problem into a more tractable baseband simulation. In this section, we will present the digital model for our receivers. We will verify our single channel receiver by testing it with gaussian noise. We will check the simulation results with analytically calculated results, and we will show that these results verify our digital computer implementation of the single channel receiver as correct. We will then test our model for the generation of the atmospheric noise samples by comparing the results in the nearly gaussian

quiet noise case with the gaussian results. These results will be similar if our implementation of the noise generator is correct. Since the noise generator is the same for all noise conditions (quiet, quiet night, tropical, and frontal), with the different conditions simulated by changing parameters only, we will then assume our noise generator is correct for all noise conditions.

The basic single channel correlation receiver model is shown in computer flow graph form in Figure 3.1. We note that we have used a rather simple integration algorithm, which is a slightly modified trapezoidal rule. We explain it as follows:

$$\frac{1}{T}\int_0^T x(t)\,dt \approx \frac{1}{T}\sum_{n=1}^{N}(x(n)+x(n-1))\frac{\Delta t}{2}, \quad (3.11)$$

where Δt is the interval between samples, $N\Delta t = T$, and $x(n)$ is a sample of $x(t)$ at time $n\Delta t$. We note that, in our case, we are integrating over one bit length, and we can only include N samples in our summation. This is because the sample called $x(N)$ for the i^{th} bit is also the sample called $x(0)$ for the $(i+1)^{th}$ bit. Since the signal on each of these bits may be different, we must assign the end point to one bit only. We therefore consider only samples $x(0)$ through $x(N-1)$ for each bit, and, in order to simplify our integrator, we assume that $x(N)$ would approximately equal $x(0)$. Thus,

$$\frac{1}{T}\sum_{n=1}^{N}(x(n)+x(n-1))\frac{\Delta t}{2} \approx \frac{1}{N}\sum_{n=0}^{N-1}x(n), \quad (3.12)$$

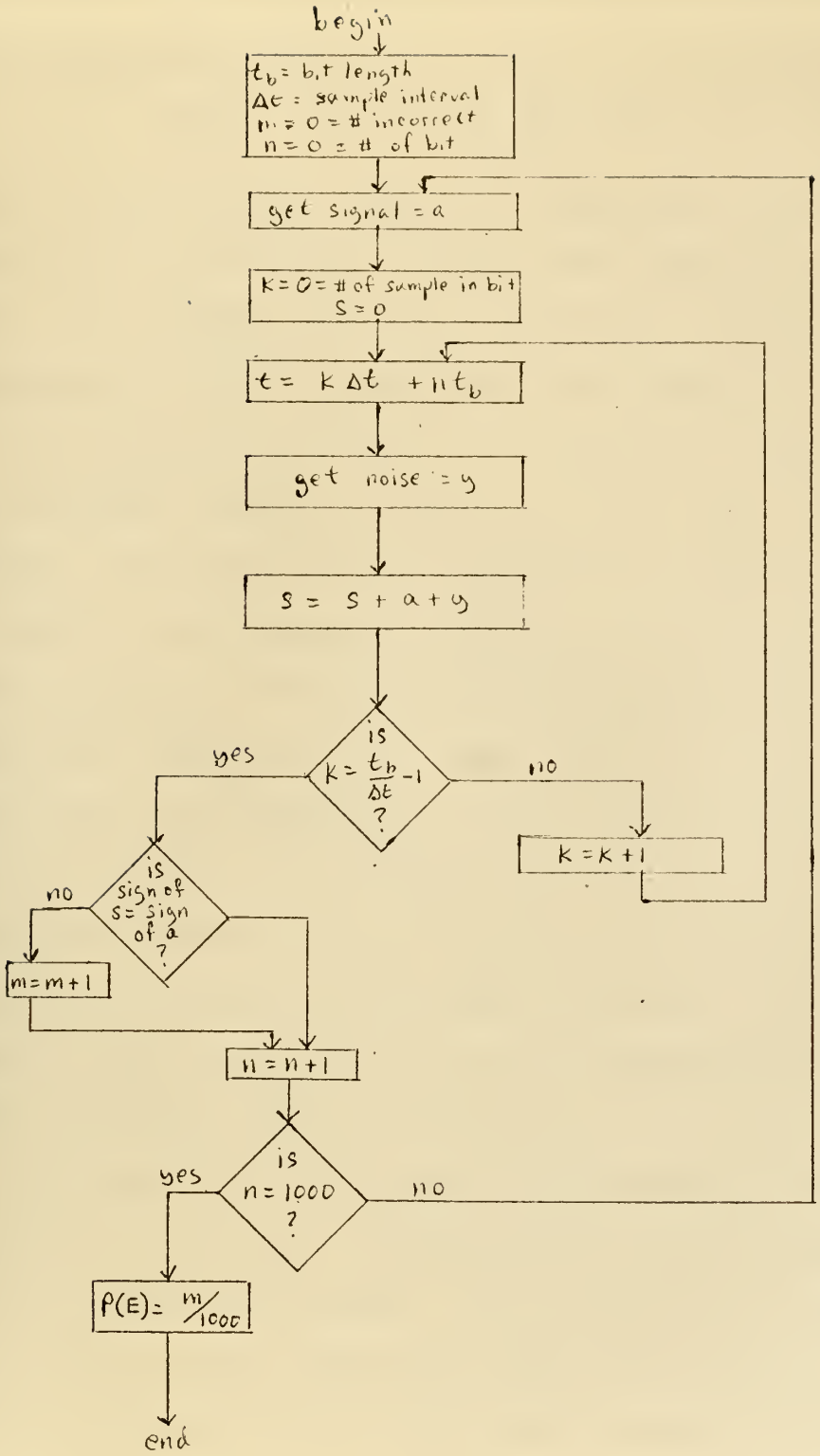

Figure 3.1 Single Channel Receiver
Computer Flow Graph

which makes our integrator

$$\frac{1}{T}\int_0^T x(t)\,dt \approx \frac{1}{N}\sum_{n=0}^{N-1} x(n), \qquad (3.13)$$

which is the slightly modified trapezoidal integration rule that we have used. We feel that when N is relatively large (for example, 40, as in our case), the errors introduced by this simplification are small.

In Figure 3.2, we show the results of a simulation of our single channel in which the noise was a gaussian process. We conducted three simulation runs of 1000 bits, at each of two bit lengths, averaged the probability of error estimates for each bit length, and plotted them versus the signal-to-noise ratio (SNR). We also calculated the probability of error for each SNR simulated, and those curves are plotted along with the corresponding simulation results. As can be seen, the calculated and experimental curves are in close agreement. We therefore conclude that our digital computer implementation of the single channel receiver is correct.

In Figure 4.4, we present the results of our simulation runs using our atmospheric noise generator with the quiet noise parameters. We note that, as we expected, the results in this case are nearly the same as in the gaussian noise case, for the single channel receiver. We feel that these results verify our implementation of

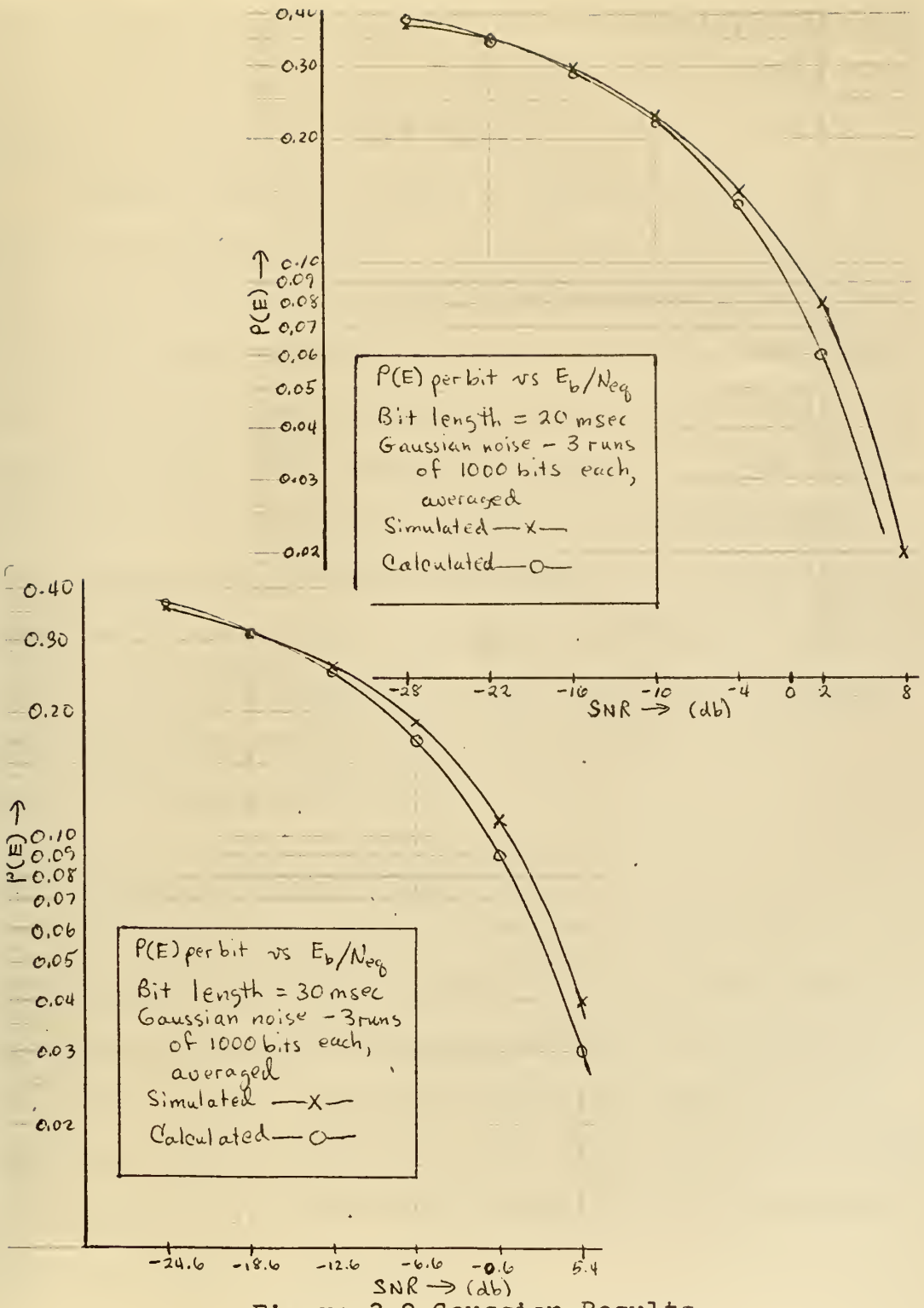

Figure 3.2 Gaussian Results

the atmospheric noise model in the quiet noise case, and hence in all other cases, since they involve simple parameter changes in the generator.

Finally, Figure 3.3 shows a computer flow graph of the dual channel receiver. We see that it is basically the same as the single channel implementation, with the exception that it incorporates the weighting function, which is based upon the second channel noise envelope samples, inside the integration routine. We feel that, since our results, shown in Figure 4.1 through Figure 4.4, indicate significant improvements in performance in the more non-gaussian noise cases and comparable performance in the nearly gaussian quiet noise case, when compared with the single channel receiver, our dual channel receiver implementation is correct.

3.3 Analog to Digital Calculations

In testing our single channel receiver versus analytically calculable results, we encountered the problem of relating the analog and digital noise power spectra. We will calculate that relationship in this section. First, however, we will show how we calculated the probability of error per binary bit of information when the noise is gaussian.[3]

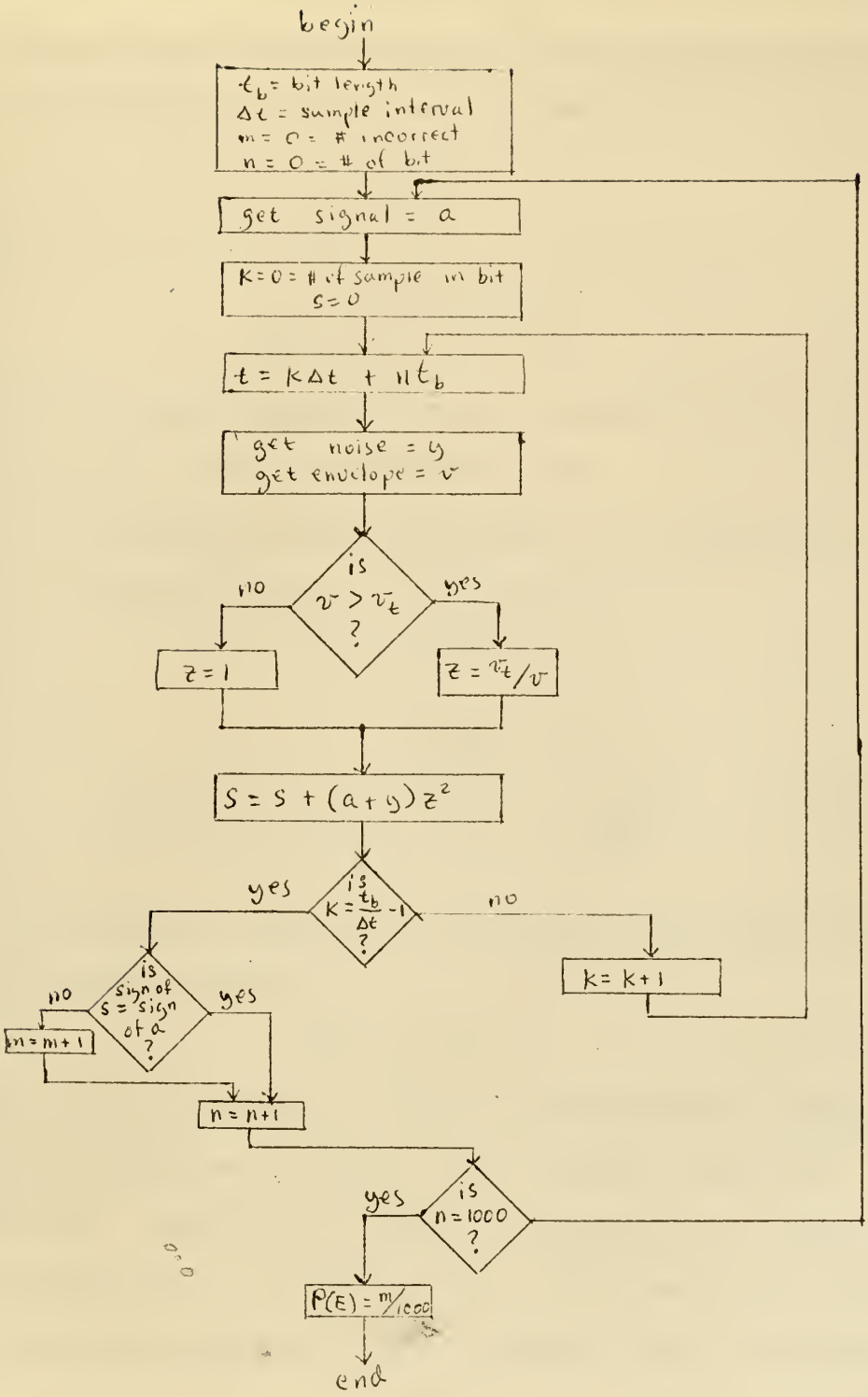

Figure 3.3 Dual Channel Receiver
Computer Flow Graph

Define the average power in the information part of the received signal, r(t), as follows:

$$P_s = E_s/T, \tag{3.14}$$

where T is the bit length and

$$E_s = \int_0^T s^2(t)\, dt, \tag{3.15}$$

where s(t) is the baseband signal portion of r(t), i.e. $s(t) = \pm A/2$. Define the source rate, R, as the rate at which binary bits are generated by the transmitter. Then, the energy per bit, E_b, is given by

$$E_b = P_s/R.$$

Therefore,

$$E_b = \frac{1/T \int_0^T s^2(t)\, dt}{R} = \frac{(A/2)^2}{R}. \tag{3.16}$$

The baseband SNR of the simulated signal and noise is defined as follows:

$$SNR = E_b/N_0, \tag{3.17}$$

where $N_0/2$ is the variance of each independent sample of the gaussian noise process in the digital computer simulation. However, in order to analytically compute the probability of error, we must obtain an expression for the power spectrum of a continuous white gaussian noise process, which is equivalent to the sampled noise process used in the simulation. We can do this in the following manner, in which n(.) represents the noise

process:[1]

Let the k^{th} noise sample be defined as

$$n(k) = \frac{1}{\Delta t} \int_0^{\Delta t} n(t)\, dt, \tag{3.18}$$

then

$$E(n^2(k)) \triangleq N_0/2 = E\left(\frac{1}{\Delta t^2} \int_0^{\Delta t}\int_0^{\Delta t} n(t_1)\, n(t_2)\, dt_1\, dt_2\right)$$

$$= \frac{1}{\Delta t^2} \int_0^{\Delta t}\int_0^{\Delta t} E(n(t_1)\, n(t_2))\, dt_1\, dt_2. \tag{3.19}$$

Recognizing that

$$E(n(t_1)\, n(t_2)) \triangleq \frac{N_{eq}}{2}\, \delta(t_1 - t_2), \tag{3.20}$$

where $\delta(.)$ is the Dirac delta function, we get

$$N_0/2 = \frac{N_{eq}/2}{\Delta t}, \tag{3.21}$$

and therefore,

$$N_{eq} = N_0 \Delta t, \tag{3.22}$$

where Δt is the time interval between samples and N_{eq} is the magnitude of the noise power spectrum of a continuous white gaussian process, analogous to the simulated process. Thus, the analog SNR corresponding to the digital SNR (equation 3.17) is given by

$$SNR = E_b/N_{eq} = E_b/N_0 \Delta t. \tag{3.23}$$

For antipodal signalling schemes, the probability of error per bit, with gaussian noise, can be calculated as follows:[3]

$$P(E) = Q\left(\sqrt{2E_b/N_{eq}}\right), \tag{3.24}$$

where $Q(x)$ is defined as

$$Q(x) = \int_x^\infty \frac{1}{2\pi} e^{-u^2/2}\, du, \qquad (3.25)$$

whose complement, 1 - Q(x), is tabulated in various references (e.g. 8). Thus, in terms of the parameters of our digital simulation, the probability of error per binary bit, with white gaussian noise, can be analytically calculated by means of the Q(.) function as

$$P(E) = Q(\sqrt{2E_b/N_0\Delta t}\,). \qquad (3.26)$$

3.4 Chapter Summary

In this chapter, we have explained why and how we converted our bandlimited receiver from a passband to a baseband system for digital simulation purposes. We went on to explain how we checked our implementations of the receiver and noise models by comparing simulated and analytical results using gaussian noise corruption and corruption by the quiet noise case of atmospheric noise. Finally, we gave the relationship between the simulated noise power spectrum and the analogous continuous power spectrum, which was necessary to calculate the probability of error per binary bit analytically.

In the next chapter, we will present the results of our simulation runs using the atmospheric noise model described in Chapter 1. We will show the averaged results for five runs of each of the four basic weather/noise conditions: quiet, quiet night, tropical, and frontal. We will show how we obtained our estimate

of P(E) per bit, and we will give bounds on that estimate. We will also give an example of the problems we encountered as we proceeded with the simulations. Finally, we will summarize the conditions under which our results were obtained so that the reader may evaluate their usefulness.

Chapter 4

SIMULATION RESULTS

Before presenting our results, we will briefly summarize our work up to this point. We discussed, in Chapter 1, bandlimited low frequency atmospheric noise, its causes, its non-gaussian nature, and a model for this noise. The model, developed by Feldman,[1] is especially suited for simulation on a digital computer. In Chapter 2, we discussed several receiver schemes, which could be used to decide which of two antipodal signals, corrupted by atmospheric noise, was transmitted. Specifically, we discussed a linear correlation receiver, which is optimum when the noise encountered is gaussian. We then discussed a design, based upon the observed properties of the non-gaussian noise, which is considerably more complicated than the simple correlation receiver, but which should yield optimum performance in the presence of this noise. Finally in Chapter 3, we discussed the problems involved with a simulation of these receivers and bandlimited low frequency atmospheric noise.

In this chapter, we present the results we obtained in our simulation of these receivers. We tested each receiver for each of four weather/noise conditions, which our noise model is capable of simulating, ranging

from the nearly gaussian quiet noise case to the extremely non-gaussian frontal noise case. For each receiver and weather/noise condition, we made five simulation runs, each run simulating the reception of 1000 bits of binary information by the receiver. In order to characterize receiver performance, we formed an estimate of the probability of error per bit of received information for each run. We then averaged the results of the five runs for each case and plotted these averages as functions of the signal-to-noise ratio of the received baseband signals.

We present a discussion of the method in which we formed our estimates of probability of error, and we give bounds upon our estimating procedure. We also bound our results by presenting tables of certain statistics of the results of the five individual runs for each case. We discuss briefly one problem we encountered during the simulation runs, and why this problem existed and how we solved it. Finally, in the last section, we present a summary of this research.

4.1 Results and Bounds

In Figures 4.1 through 4.4, we have plotted the results of our simulation runs for frontal, tropical, quiet night, and quiet weather/noise conditions, respectively. The curves shown are plotted on semi-log

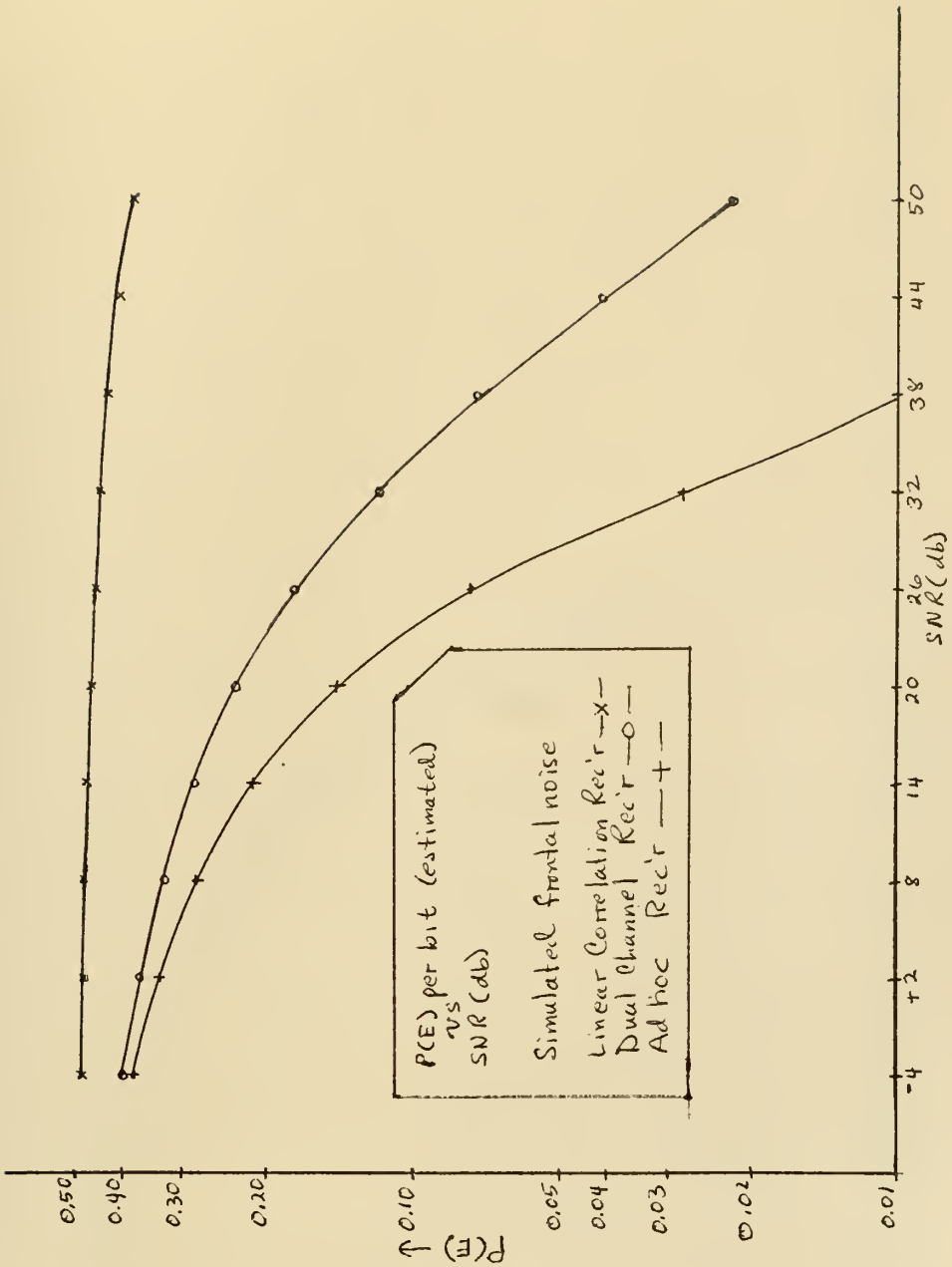

Figure 4.1 Frontal Noise

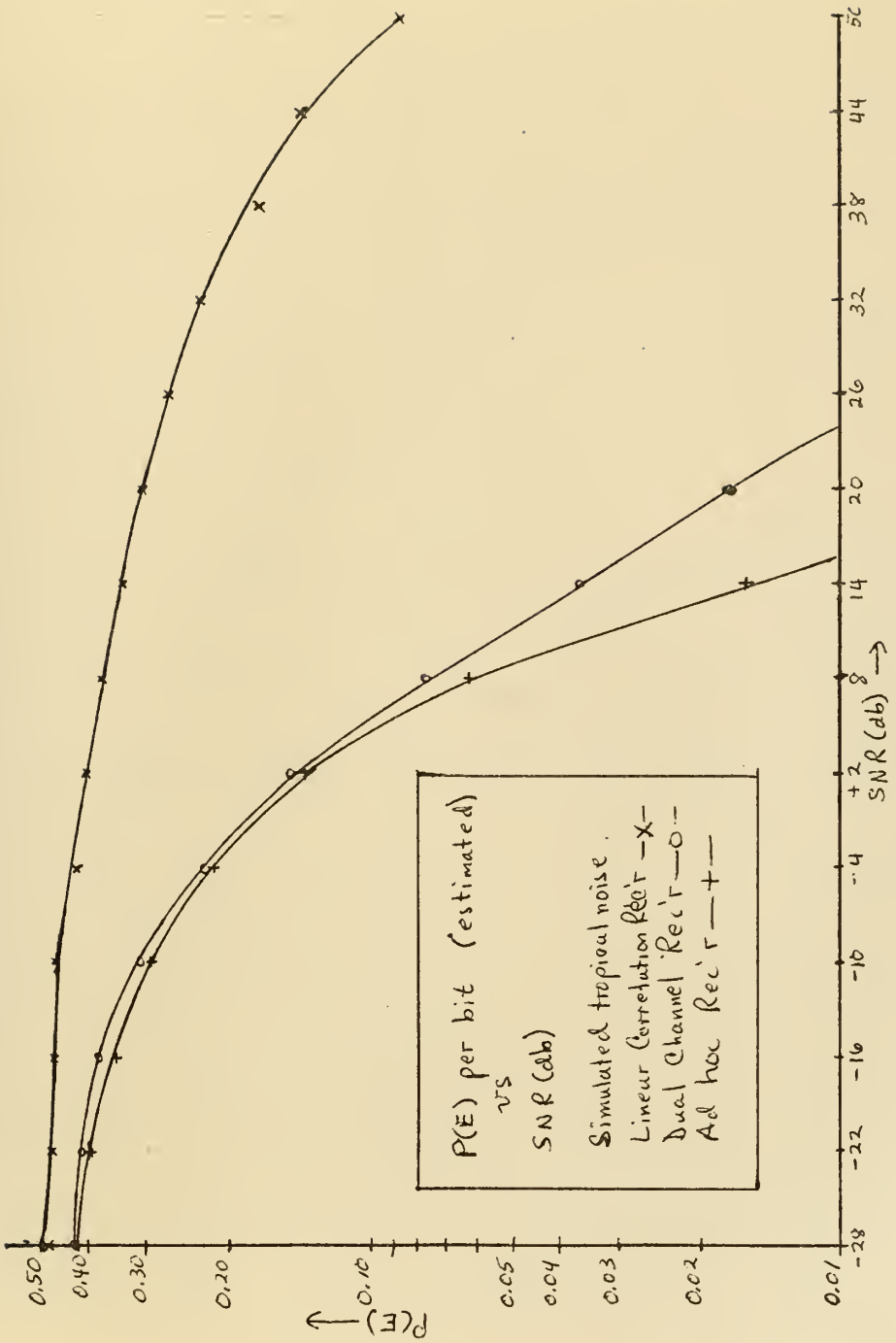

Figure 4.2 Tropical Noise

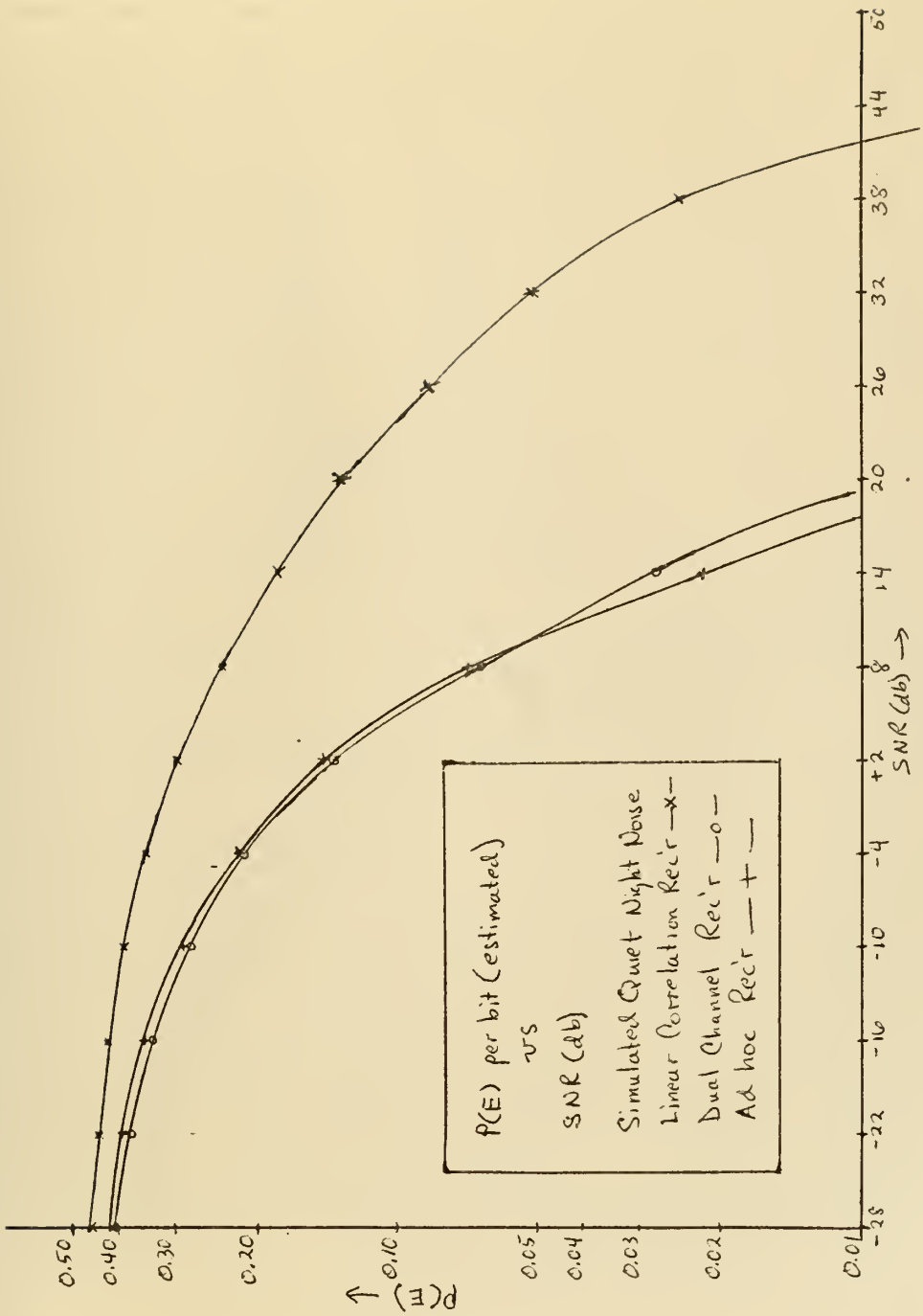

Figure 4.3 Quiet Night Noise

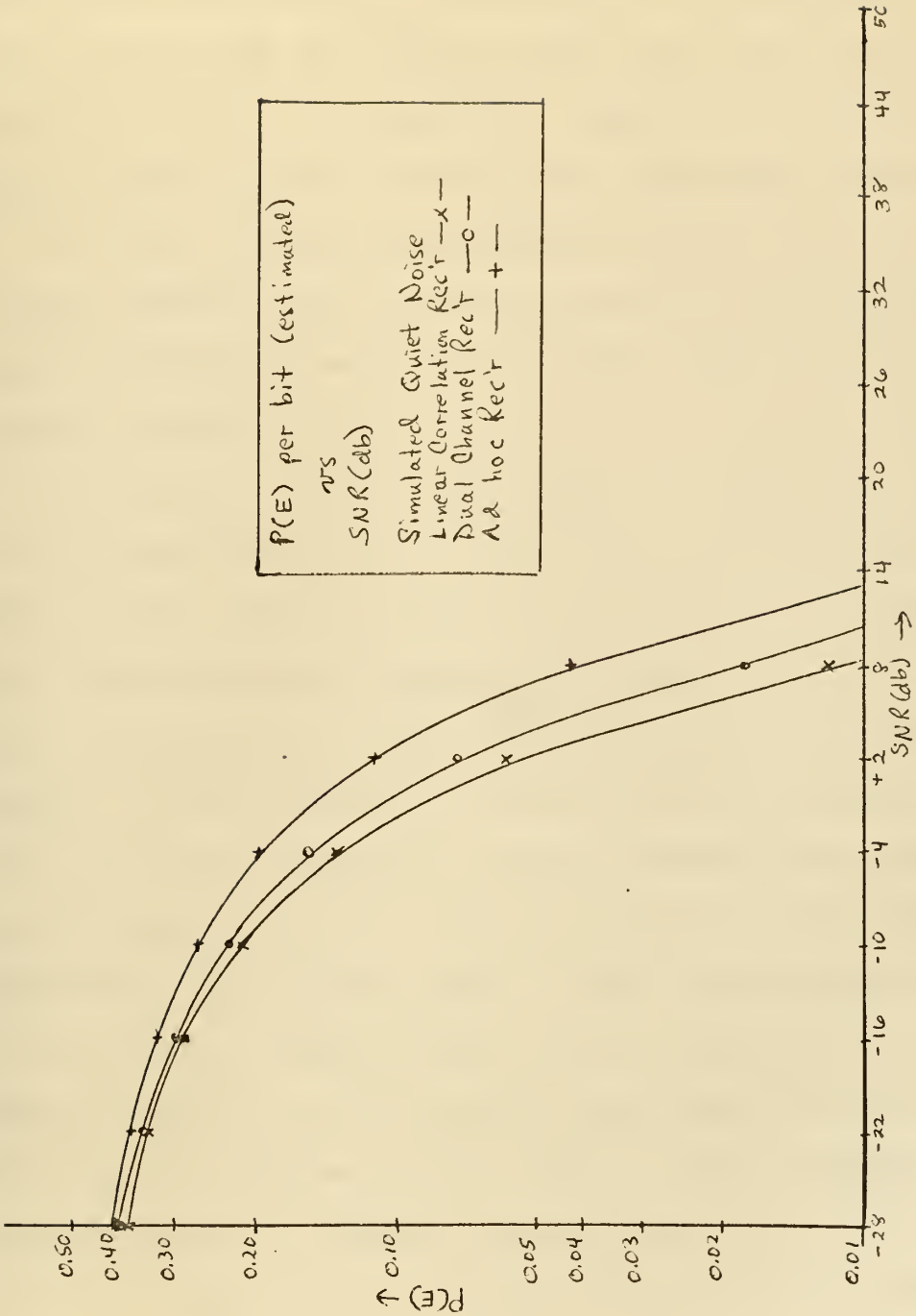

Figure 4.4 Quiet Noise

paper, with the ordinate representing the probability of error per bit and the abcissa being the signal-to-noise ratio in decibels (20 log SNR). There are three curves shown in each figure. These curves represent the results of the single channel correlation reciever, the dual channel receiver, and the ad hoc receiver (described in Section 2.3) which we used as a check upon our dual channel receiver.

The curves shown in each graph represent the average of five simulation runs of 1000 bits of received information each. The bit length for all runs was 20 msec, making the simulated length of each run 20 seconds. The signal-to-noise ratio scale was defined in the following manner: It is necessary to realize that the noise power level is vastly different from one weather/noise condition to any other. However, the bandlimited low frequency atmospheric noise model used in these simulations consists of two linearly combined functions, a background low level gaussian process, and a process which represents the high energy burst behavior of the noise.[1] The background gaussian noise is assumed to have been generated in the receiver itself (receiver front-end noise),[2] and therefore, it is independent of the particular weather/noise condition being simulated. Since we would like our SNR scale to be independent of the weather/noise condition being

simulated, we base it upon the signal power and the power level of the background gaussian process.

Thus, our SNR is given by equation 3.23, which is repeated here:

$$SNR = E_b/N_0\Delta t,$$

where E_b is the energy per bit, as given by equations 3.14 through 3.16, $N_0/2$ is the variance of each independent sample of the background gaussian noise process of our noise model (all the parameters of our noise model have been normalized such that $N_0/2 = 1$),[1] and Δt is the sampling interval.

The estimate of the probability of error per bit was formed by counting the number of incorrect decisions made by the receiver and dividing that number by the total number of bits simulated. For example, in a run where we simulated 1000 bits, and where the receiver made 351 incorrect decisions (we have assumed that the probability of making an error is independent of the signal, either a binary one or a binary zero, which was sent), our estimate of the probability of error per bit in that run would be 0.351.

We now present an evaluation of our estimation procedure. First, we assume that the probability that an error is made on any particular bit, for any particular receiver and weather/noise condition, is

constant and can be denoted by the value p. Then the probability that a correct decision is made on any bit is simply (1 - p). We assume that the decision made on each bit is independent of any, and all, other bits.

Now we can assign a random variable, say k_i, to the outcome of the i^{th} decision of the receiver. The random variable, k_i, is defined to have the following probability density function:

$$P(k_i = 0) = 1 - p, \tag{4.1a}$$

$$P(k_i = 1) = p. \tag{4.1b}$$

Therefore, we see that k_i is one if, and only if, an error is made on the i^{th} bit, and k_i is zero otherwise. Now we define the random variable s, such that

$$s = 1/N \sum_{i=1}^{N} k_i, \tag{4.2}$$

where N is the number of bits simulated. We know that the set of k_i is a set of independent identically distributed random variables, each having the probability density function given in equations 4.1 above, which we note is the well defined binomial density. Therefore, the mean and variance of each k_i are given below:[8]

$$E(k_i) = p, \tag{4.3}$$

$$\begin{aligned} Var(k_i) &= p\ (1 - p) \\ &= p - p^2. \end{aligned} \tag{4.4}$$

Now, we see that, by the central limit theorem, if N is

large, the probability density function for s is gaussian with mean and variance described by

$$E(s) = E(1/N \sum_{i=1}^{N} k_i)$$

$$= 1/N \sum_{i=1}^{N} E(k_i)$$

$$= p, \qquad (4.5)$$

and

$$Var(s) = E(s^2) - (E(s))^2$$

$$= E(1/N^2 \sum_{i=1}^{N} \sum_{j=1}^{N} k_i \, k_j) - p^2$$

$$= (p - p^2)/N, \qquad (4.6)$$

where we have used the independence of the k_i. We make note of the facts that s is an unbiased estimate of p, and that the variance of s decreases toward zero as the number of bits simulated increases.

Finally, in order to establish a bound upon our estimates of probability of error per bit, as given by s in equation 4.2, we used a table[8] of the complement of the Q(.) function, described in equation 3.25. We note from the table that, with 95% confidence, our estimate of the probability of error per bit will be within two standard deviations of the actual value. We also note that the variance of our estimate, and hence its standard deviation, is greatest when the actual value of p is 0.5. We therefore use this case for a

worst case analysis of our estimation procedure.

When p = 0.5, the variance of s is

$$\text{Var}(s) = (0.5 - 0.25)/N = 0.25/N. \qquad (4.7)$$

In our case, we have made five runs of 1000 bits each; thus making N = 5000. Therefore,

$$\text{Var}(s) = 0.25/5000, \qquad (4.8)$$

and the standard deviation, σ_s, is

$$\sigma_s = \sqrt{0.25/5000} = 0.00708, \qquad (4.9)$$

and thus,

$$2\sigma_s = 0.01416. \qquad (4.10)$$

From the above, we can see that, with 95% confidence, our estimates of the actual probability of error per binary bit should be within less than $\pm$ 0.014 of the actual values. As a matter of practical concern, we note that each run of 1000 simulated bits of information was conducted independently of the others. We therefore also present a summary of the results of the five runs for each weather/noise condition and receiver. These results are presented in tabular form in Tables 4.1 through 4.4. In these tables, we give the average of probabilities of error of the five runs for each case and the maximum deviation from that average.

4.2 Difficulty

The most serious difficulty encountered in this research was an apparent breakdown in our single channel

	single channel		dual channel		ad hoc	
SNR(db)	P(E) average	max. dev.	P(E) average	max. dev.	P(E) average	max. dev
-28	no data		no data		no data	
-22	no data		no data		no data	
-16	no data		no data		no data	
-10	no data		no data		no data	
-4	0.488	0.022	0.398	0.015	0.379	0.009
+2	0.486	0.023	0.370	0.009	0.334	0.023
8	0.483	0.024	0.330	0.009	0.281	0.015
14	0.477	0.021	0.285	0.012	0.215	0.022
20	0.469	0.021	0.234	0.018	0.145	0.011
26	0.459	0.023	0.177	0.019	0.077	0.009
32	0.450	0.024	0.119	0.019	0.028	0.005
38	0.435	0.023	0.075	0.014	0.007	0.005
44	0.412	0.021	0.041	0.007	0.001	0.001
50	0.384	0.022	0.022	0.005	0.000	0.000

Table 4.1 Frontal Noise

	single channel		dual channel		ad hoc	
SNR(db)	P(E) average	max. dev.	P(E) average	max. dev.	P(E) average	max. dev.
-28	0.482	0.010	0.422	0.025	0.419	0.028
-22	0.476	0.010	0.393	0.023	0.384	0.021
-16	0.465	0.011	0.353	0.017	0.345	0.022
-10	0.449	0.021	0.291	0.025	0.288	0.013
-4	0.425	0.035	0.226	0.027	0.215	0.022
+2	0.401	0.045	0.149	0.021	0.139	0.017
8	0.374	0.042	0.077	0.018	0.062	0.013
14	0.341	0.053	0.036	0.011	0.016	0.012
20	0.306	0.056	0.017	0.003	0.002	0.003
26	0.270	0.052	0.007	0.004	0.000	0.000
32	0.231	0.044	0.004	0.003	0.000	0.000
38	0.183	0.034	0.002	0.002	0.000	0.000
44	0.140	0.030	0.001	0.001	0.000	0.000
50	0.087	0.023	0.000	0.000	0.000	0.000

Table 4.2 Tropical Noise

SNR(db)	single channel P(E) average	single channel max. dev.	dual channel P(E) average	dual channel max. dev.	ad hoc P(E) average	ad hoc max. dev.
-28	0.462	0.031	0.407	0.022	0.422	0.033
-22	0.446	0.026	0.378	0.019	0.391	0.035
-16	0.423	0.035	0.333	0.022	0.349	0.027
-10	0.393	0.037	0.280	0.017	0.292	0.023
-4	0.352	0.030	0.214	0.018	0.218	0.022
+2	0.302	0.038	0.139	0.021	0.146	0.020
8	0.241	0.040	0.067	0.016	0.071	0.020
14	0.183	0.038	0.028	0.011	0.022	0.011
20	0.134	0.031	0.008	0.010	0.003	0.002
26	0.088	0.014	0.002	0.003	0.000	0.000
32	0.052	0.011	0.000	0.001	0.000	0.000
38	0.025	0.008	0.000	0.000	0.000	0.000
44	0.005	0.004	0.000	0.000	0.000	0.000
50	0.001	0.001	0.000	0.000	0.000	0.000

Table 4.3 Quiet Night Noise

SNR(db)	single channel P(E) average	single channel max. dev.	dual channel P(E) average	dual channel max. dev.	ad hoc P(E) average	ad hoc max. dev.
-28	0.383	0.026	0.395	0.020	0.404	0.026
-22	0.346	0.026	0.353	0.021	0.374	0.029
-16	0.288	0.023	0.298	0.023	0.332	0.022
-10	0.215	0.026	0.232	0.026	0.270	0.026
-4	0.136	0.021	0.155	0.027	0.199	0.026
+2	0.059	0.014	0.075	0.012	0.114	0.017
8	0.012	0.004	0.018	0.006	0.043	0.011
14	0.001	0.001	0.002	0.001	0.006	0.002
20	0.000	0.000	0.000	0.000	0.000	0.001
26	0.000	0.000	0.000	0.000	0.000	0.000
32	0.000	0.000	0.000	0.000	0.000	0.000
38	0.000	0.000	0.000	0.000	0.000	0.000
44	0.000	0.000	0.000	0.000	0.000	0.000
50	0.000	0.000	0.000	0.000	0.000	0.000

Table 4.4 Quiet Noise

linear correlation receiver model. Our original intention was to make only one simulation run, of 1000 bits, for each receiver and weather/noise condition while varying both signal magnitude and bit length. We note that an increase in either signal magnitude or bit length results in an increase in SNR, and therefore should result in a decrease in the probability of error per bit. For our dual channel receiver, this was indeed the case, but with the single channel model, we found that the probability of error was increasing slightly with increasing bit length for all signal magnitudes below a certain, non-constant threshold.

We reasoned that it would be interesting to see how well each receiver performed as a function of both the signal magnitude and the bit length. Therefore, we thought that we were keeping all other factors constant and varying only the factor of interest, either the bit length or the signal magnitude, from run to run. We must diverge here slightly and explain the manner in which we generate the noise process upon a digital computer. To generate any random process upon a digital computer, we in fact are generating a sequence of pseudorandom numbers, these numbers being samples of the noise process. In order to generate this sequence, we must initialize all random number generators in the computer program (see Figure 1.1). Furthermore, if we

initialize all the random number generators the same way in every run of the same program, we will generate the identical random number sequence.[9]

Now we can see that when we varied the signal magnitude only, and kept the bit length constant, the noise process which corrupted each bit was the same for all signal magnitudes since we initialized all random numbers in the same manner at the start of each run. However, when we varied the bit length, while keeping the signal magnitude constant, the noise process seen by each bit changed radically with bit length, regardless of how we initialized the random number generators. Thus, we were varying two factors, both the noise process and the bit length. We made several more runs, with different initial conditions upon the random number generators, and we found that the probability of error did indeed decrease as we increased bit length in these runs. We therefore reasoned that our first run had been made with a non-typical noise process that caused the probability of error to increase slightly with increasing bit length.

We subsequently decided that we should make several runs, starting with different initial conditions upon the random number generators each time, for each bit length and each signal magnitude. However, due to time constraints, we found that we could only make several runs for each weather/noise condition, receiver, and

signal magnitude at one bit length. We feel that in this way our results are typical of the actual results to be expected for that bit length. We chose a bit length of 20 msec, about the shortest bit length practical in low frequency digital communication systems,[1] because it resulted in the shortest time per simulation run.

4.3 Summary of Research Conditions

In this section, we present a summary of the receiver and noise models we used in the simulation runs which we made. We also give a short summary of the results we obtained.

The model for bandlimited low frequency atmospheric noise which we used was developed by Feldman.[1] This noise model accurately models the first order statistics and the time structure of the actual bandlimited noise waveform for four weather/noise conditions. These four conditions include the nearly gaussian quiet noise case, the quiet night noise case, the tropical noise case, and the most severe frontal noise case. These four conditions model noise which is typical of large of areas of the world over significantly large periods of time. The quiet noise conditions exist when the atmsophere in the vicinity of the receiver consists of a stable air mass. The tropical conditions exist when the air is warm, moist, and unstable. Quiet night conditions represent a

transitional period between quiet and tropical conditions. And, of course, frontal noise conditions, the most violent conditions, exist when there is a front, with much thunderstorm activity, in the vicinity of the receiver. A canonic noise generator, useful in computer simulations, and a table of associated parameters are given in Figure 1.1 and Table 1.1 of this work.

For our simulation, we chose binary antipodal signalling, with a coherent PSK modem. The carrier frequency of our signals was 65 kHz and the receiver's bandlimiting filters had a bandwidth of 1 kHz. We also measured the noise envelope on a second frequency channel, with bandwidth 1 kHz, centered at 83 kHz. These frequencies were chosen because they are typical of digital communication systems, and we have the parameters for simulation of the noise model at these frequencies.[1]

As a standard of comparison, we simulated a single channel linear correlation receiver, using a 20 msec bit length, operating in the above described low frequency atmospheric noise. Our test statistic, an estimate of the receiver's probability of error per binary bit, was calculated simply by counting the number of incorrect decisions made by the receiver and dividing by the number of bits simulated. We made five runs, of 1000 bits each, for each weather/noise condition for various signal-to-noise ratios.

We then tested, in a similar manner, a dual channel receiver which uses the fact that, above a certain threshold, the value of the noise envelope on the 83 kHz channel and the value of the noise waveform on the signal channel are statistically dependent. Due to the sampling rates involved, and limitations of the noise model, we simulated both of the above receivers in the baseband rather than the passband.

We found that this dual channel receiver performed better than the single channel receiver for the three worst noise conditions (frontal, tropical and quiet night), and as the signal-to-noise ratio increased, the performance improvement exceeded an order of magnitude. However, in the quiet noise case, we found that the dual channel receiver yielded approximately the same performance as the single channel model.

4.4 Chapter Summary

In this chapter, we have presented our results of the simulations of the single and dual channel receivers. We also presented an analysis of the estimate of probability of error per bit which we used, and we gave bounds upon our results. We explained a difficulty we encountered in the course of the simulations, and we explained how we overcame it. Finally, we presented a summary of the research reported in this work. In the next chapter, we present our conclusions and ideas for further research.

Chapter 5

CONCLUSIONS AND SUGGESTIONS FOR FURTHER RESEARCH

We first present a brief summary of this research. In Chapter 1, we described low frequency atmospheric noise and a model for this noise. In Chapter 2, we presented two receiver designs: a linear correlation receiver, the optimum receiver when the noise corrupting the signal is gaussian; a dual channel design, based upon the observed non-gaussian characteristics of bandlimited low frequency atmospheric noise, which should be optimum for this noise. In Chapter 3, we presented the calculations necessary to relate the digital simulation to the analog system being modelled. In Chapter 4, we presented our results for the two receivers described above, and some bounds upon those results. In this chapter, we will give our conclusions based upon our results, and we will also give some suggestions for further research with the dual channel receiver design.

5.1 Conclusions

Our results, shown in graphical form in Figures 4.1 through 4.4, were favorable. We found that the dual channel receiver yielded significant performance improvements over the single channel receiver in the three more

violent weather/noise conditions (frontal, tropical, and quiet night). In the nearly gaussian quiet noise condition, the dual channel receiver performed approximately the same as the single channel linear receiver. The performance improvements in the more violent noise cases were more than an order of magnitude as the signal-to-noise ratio increased.

The results were as we expected. We note that the single channel linear correlation receiver is the optimum gaussian receiver, and it tends to be optimum in the quiet noise case. However, as the noise becomes more non-gaussian, we note that the dual channel receiver performs much better. Finally, in the frontal noise case, the most violent noise case, the single channel receiver could do little better than guess, while the dual channel receiver made correct decisions with about 98% confidence at the same signal-to-noise ratio.

We therefore conclude that the dual channel receiver, while being approximately twice as complicated as the single channel receiver, yielded a significant improvement and should be investigated further. It must be noted that we have simulated only the simplest case, using coherent PSK signals, but we feel that our results indicate that the dual channel receiver design is a potentially powerful design for low frequency digital communication systems.

5.2 Suggestions for Further Research

We have tested our dual channel receiver design against the optimum receiver for gaussian noise, but we have not tested it against a receiver which is more similar to those currently used to receive signals corrupted by non-gaussian atmospheric noise. Practical correlation receiver designs for use in low frequency signalling systems use nonlinear devices, placed before the integrator, to limit the effects of the non-gaussian high energy noise bursts. Typical nonlinear devices which are used, or suggested for use, are clippers, limiters, and hole punchers.[1,2] (see Figure 5.1)

We suggest that a possible research program, based upon our results, would be to determine the optimum nonlinear device to be placed in the single channel receiver, and to determine the optimum point at which limiting, or attenuating, occurs. Simulations could be run, using this optimum nonlinear receiver, and the results compared with the results we have obtained with the dual channel receiver. Since the single channel, nonlinear receiver would be simpler to implement than the dual channel design, it would be interesting to determine how much performance improvement, if any, is possible with the dual channel design over the single channel nonlinear design.

In our research, we assumed we had phase coherent

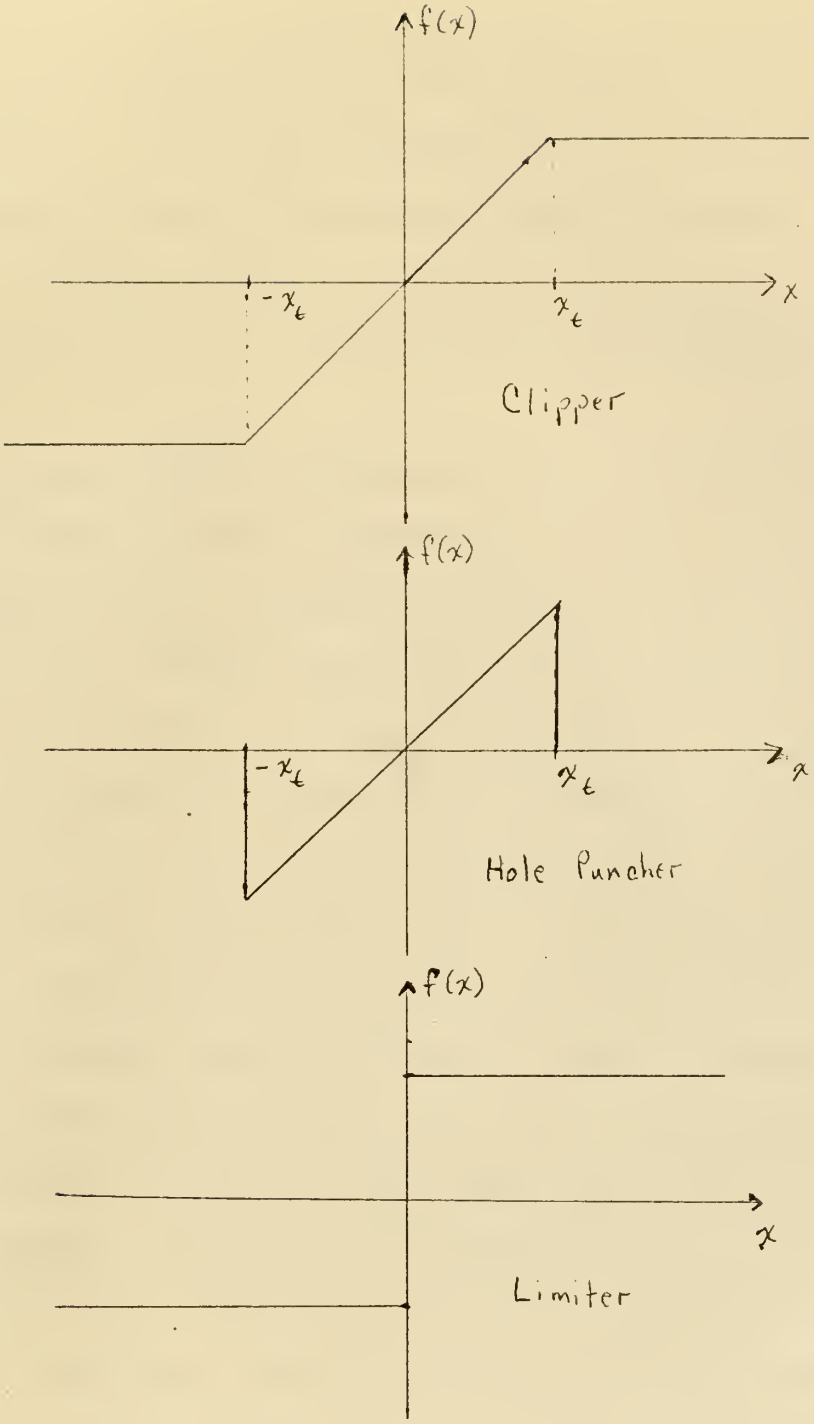

Figure 5.1 Nonlinear Devices

receivers, and we postulated that the results we obtained would give an indication of the performance to be expected in the case of incoherent receivers. Several standard communication theory references (e.g. 3,4) could be used to find implementations of incoherent receivers, and the test we made could be redone using these incoherent receivers.

We found several references to an incoherent receiver design[5,6] which uses a combination of energy detection and a pilot tone to determine the phase of the received signal. This receiver has been simulated and results have been presented for the case in which the corrupting noise is gaussian.[5] It would be interesting to implement this receiver in a dual channel design, and to test it in the presence of the non-gaussian atmospheric noise.

The information from the second channel can also be used in an error detection scheme. Since the noise has a time varying power level, the actual signal-to-noise ratio for each bit of received signal may fluctuate. The second channel noise envelope measurements can be used to determine the actual signal-to-noise ratio on any bit, and when the actual SNR is below a certain threshold, the receiver can indicate that the bit is probably in error.[1]

Since we found that the single channel receiver is indeed the optimum receiver during the quiet noise

periods, while the dual channel receiver performs much better in the more severe noise periods, it would be convenient to have some device which determines when to switch between the single and dual channel receivers. Furthermore, the thresholds for the dual channel design vary with the particular weather/noise condition in existence. Therefore, it would be beneficial to design an algorithm which samples the noise envelope on the second channel and determines which receiver and/or which threshold (v_t, from equation 2.16) value to use.

BIBLIOGRAPHY

1. Feldman, D. A., "An Atmospheric Noise Model with Application to Low Frequency Navigation Systems," Sc. D. Thesis, Massachusetts Institute of Technology (unpublished), June 1970.

2. Beach, C. D. and D. C. George, "Error Performance of VLF and LF Receiving Systems with Nonlinear Atmospheric Noise Reduction," Westinghouse Electric Corp. Report RADC-TR-70-190, AD-875-991, September 1970.

3. Wozencraft, J. M. and I. M. Jacobs, Principles of Communication Engineering, J. Wiley and Sons, New York, 1967.

4. Van Trees, H. L., Detection, Estimation, and Modulation Theory, Part I, J. Wiley and Sons, New York, 1968.

5. Olsen, R. G., "Simulation of a Binary Phase-Shift-Keying Communication System," S. M. Thesis, Massachusetts Institute of Technology (unpublished), September 1968.

6. Van Trees, H. L., "Optimum Power Division in Coherent Communication Systems," IEEE Transactions on Space Electronics and Telemetry, SET-10, Nr 1, March 1964.

7. Viterbi, A. J., Principles of Coherent Communication, McGraw-Hill, New York, 1966.

8. Drake, A. W., Fundamentals of Applied Probability Theory, McGraw-Hill, New York, 1967.

9. Reitman, J., Computer Simulation Applications, J. Wiley and Sons, New York, 1971.